Biological Electrocatalysts

Deutsche Ausgabe: DOI: 10.1002/ange.201602627
Internationale Ausgabe: DOI: 10.1002/anie.201602627

Bioreduction of Precious Metals by Microorganism: Efficient Gold@N-Doped Carbon Electrocatalysts for the Hydrogen Evolution Reaction

Weijia Zhou, Tanli Xiong[+], Chaohong Shi[+], Jian Zhou, Kai Zhou, Nengwu Zhu,* Ligui Li, Zhenghua Tang, and Shaowei Chen*

Abstract: *The uptake of precious metals from electronic waste is of environmental significance and potential commercial value. A facile bioreductive synthesis is described for Au nanoparticles (ca. 20 nm) supported on N-doped carbon (Au@NC), which was derived from Au/Pycnoporus sanguineus cells. The interface and charge transport between Au and N-doped carbon were confirmed by HRTEM and XPS. Au@NC was employed as an electrocatalyst for the hydrogen evolution reaction (HER), exhibiting a small onset potential of −54.1 mV (vs. RHE), a Tafel slope of 76.8 mV dec^{-1}, as well as robust stability in acidic medium. Au@NC is a multifunctional electrocatalyst, which demonstrates high catalytic activity in the oxygen reduction reaction (ORR), as evidenced by an onset potential of +0.97 V, excellent tolerance toward methanol, and long-term stability. This work exemplifies dual recovery of precious Au and fabrication of multifunctional electrocatalysts in an environmentally benign and application-oriented manner.*

Over the past decade, hydrogen has attracted attention as a clean and renewable energy because of its high calorific value and eco-friendliness. The electrocatalytic hydrogen evolution reaction (HER) is one of the most important methods for hydrogen production that may efficiently store energy from renewable sources in large scale, thereby meeting the massive global demand for clean energy.[1] Transition metal carbides,[2] sulfides,[3] phosphides,[4] and composites,[5] have been intensively investigated as HER catalysts. Recent studies show that active carbon-based materials (for example, metal@carbon) are efficient hydrogen evolving catalysts.[6] Bao et al. reported that CoNi metal particles wrapped in ultrathin graphene layers significantly promoted electron penetration and enhanced the activity of the HER. The catalytically active sites were primarily located at the carbon atoms, and it was possible to modulate the electronic state density of these sites with the adjacent transition-metal elements.[7]

Au nanoparticles as electrocatalysts for the oxygen reduction reaction (ORR)[8] and the oxygen evolution reaction (OER)[9] have been widely studied. Yan et al. reported that Au nanoparticles occupying the core of Au@Co_3O_4 core–shell nanocrystals with uniform particle size and shell thickness, exhibited enhanced OER activity because of the synergistic effect between the core and the shell. However, to the best of our knowledge, Au nanoparticles as HER electrocatalysts are rare.[10] More importantly, recovery and reuse of precious metals (such as Au and Ag) derived from waste electronic equipment (such as mobile phones) is of environmental significance, and holds great potential for industrial commercialization.[11] Das and Marsili et al. successfully prepared Au nanoparticles by bioreductive synthesis in *R. oryzae* cells; the biosynthetic process was considered economically viable and environmentally friendly.[11b]

Herein, we describe a fusion of the concepts of precious metal recovery and fabrication of metal@carbon core–shell structures: from waste (Au/microorganism) to wealth (Au@NC as electrocatalysts for HER and ORR), as shown in Figure 1. Firstly, an Au^{3+} aqueous solution (used to simulate the Au^{3+} leachate of electronic equipment) was mixed with *Pycnoporus sanguineus* cells (Supporting Information, Figure S1a,b). The hue of the solution gradually became yellow upon diffusion of Au^{3+} into the microorganism (Supporting Information, Figure S2). Subsequently, blue aggregates of the Au/microorganism composite formed at the bottom of the solution, indicating the reduction of Au^{3+} into Au nanoparticles (Supporting Information, Figure S1c,d). The Au^{3+} ions were either trapped on the cell wall by electrostatic interactions, or fully diffused and penetrated into the cytoplasm. Subsequently, the ions were reduced by proteins/enzyme to form Au nanoparticles.[11b]

[*] Prof. W. Zhou, T. Xiong,[+] C. Shi,[+] K. Zhou, Prof. N. Zhu, Prof. L. Li, Prof. Z. Tang, Prof. S. Chen
School of Environment and Energy, South China University of Technology, Guangzhou Higher Education Mega Center
Guangzhou, Guangdong 510006 (China)
E-mail: eszhouwj@scut.edu.cn
nwzhu@scut.edu.cn
Prof. J. Zhou
National Laboratory of Solid State Microstructures and Department of Materials Science and Engineering, Nanjing University
Nanjing, Jiangsu 210093 (China)
Prof. W. Zhou, Prof. N. Zhu
Guangdong Provincial Key Lab of Atmospheric Environment and Pollution Control, Environmental Protection Key Lab of Solid Waste Treatment and Recycling, Key Lab of Pollution Control and Ecosystem Restoration in Industry Clusters, Ministry of Education, South China University of Technology, Guangzhou Higher Education Mega Centre
Guangzhou 510006 (China)
Prof. S. Chen
Department of Chemistry and Biochemistry, University of California
1156 High Street, Santa Cruz, CA 95064 (USA)
[+] These authors contributed equally to this work.

Supporting information for this article can be found under: http://dx.doi.org/10.1002/anie.201602627.

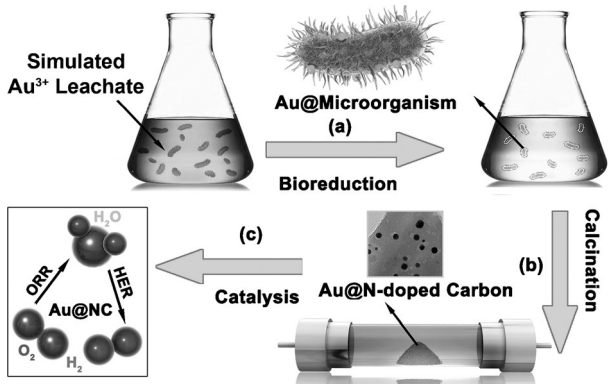

Figure 1. Electrocatalyst preparation by adsorption of gold ions, in situ bioreduction by microorganism, and conversion into Au@NC by calcination under Ar atmosphere.

Finally, the Au/microorganism composite was calcined under Ar atmosphere to obtain Au@NC, which was employed as an efficient electrocatalyst for HER and ORR. The TEM image and a photo of the precious Au reclaimed from Au@NC are shown in Figure S3 (Supporting Information). The purification temperature under air atmosphere was identified as 550 °C by differential thermal analyzer and thermal gravimetric analysis (DTA/TG; Supporting Information, Figure S4).

The fibrous morphology of Au@NC (Figure 2a) was examined by SEM, showing Au nanoparticles as bright dots on the carbon support (Figure 2a,b). TEM was employed to further characterize the strong interactions between Au and NC. Au nanoparticles 10–40 nm in diameter were loaded on the carbon substrate with different contrasts (Figure 2c; Supporting Information, Figure S5). The nanoparticles exhibited clearly defined lattice fringes with a spacing of 0.235 nm that was consistent with the (111) crystalline planes of Au (Figure 2d). Meanwhile, the carbon layer on the surface of the Au core exhibited apparent lattice fringes with a spacing of 0.34 nm, which can be attributed to graphite (002) planes. Notably, an intimate contact was observed between the Au core and carbon shell, which is possibly due to chemical interactions between elements (Supporting Information, Figure S6). Furthermore, as presented in EDX elemental mapping (Figure 2e), nitrogen was evenly distributed throughout the carbon substrate, and Au nanoparticles were well-dispersed as discrete dots within the N-doped carbon.

The successful incorporation of Au into a carbon support derived from a microorganism was confirmed by XRD (Figure 3a). Notably, a broad peak associated with the carbon support shifted positively from 28° (NC) to 30.2° (Au@NC), implying Au-promoted graphitization of carbon. Additionally, the large I_D/I_G apparent in the Raman spectra indicate that a variety of defects are present in the carbon support of Au@NC (Figure 3b). XPS measurements were carried out to determine the elemental compositions and valence states of Au@NC. Deconvolution of the high resolution scanning peak of the N 1s electrons yielded three peaks at 398.5, 400.5, and 401.3 eV (Figure 3c), which were assigned to pyridinic-N, pyrollic-N, and graphitic-N,

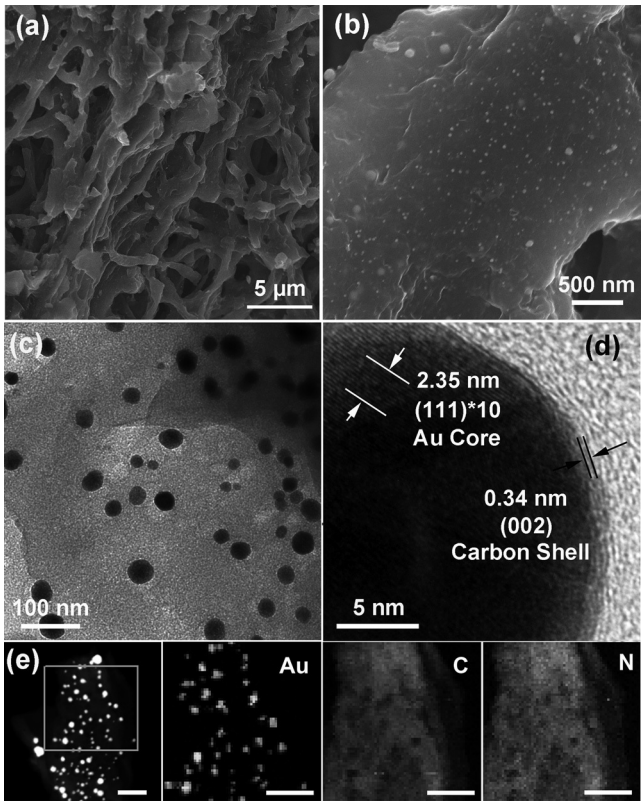

Figure 2. a) and b) SEM images; c) and d) TEM images; e) EDX elemental mapping images of Au, C, and N in Au@NC. Scale: 200 nm.

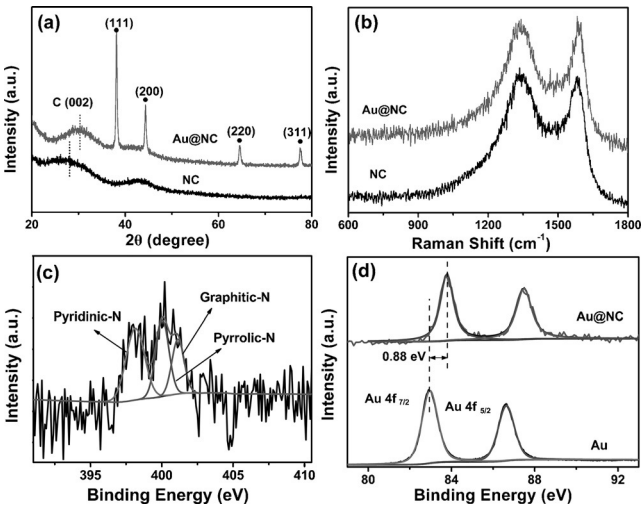

Figure 3. a) XRD patterns; b) Raman spectra; c) and d) XPS survey spectrum of N (c) and Au (d) in Au@NC.

respectively, indicating the successful incorporation of N into the carbon support. Figure 3d displays the Au 4f spectra for Au@NC, where two peaks at 83.7 and 87.5 eV can be assigned to Au^0 $4f_{7/2}$ and $4f_{5/2}$ photoelectrons, respectively. However, this binding energy shifted about 0.88 eV in the positive direction compared to pure Au nanoparticles, suggesting that electron transfer occurs from the Au core to

the NC shell. This observation is consistent with a previous report describing the enhanced catalytic activity promoted by gold nanoparticles.[12] Based on the integrated peak areas, the Au and N atomic content in Au@NC were estimated to be 0.47 at% (7.8 wt%) and 3.2 at% (3.6 wt%), respectively.

The HER electrocatalytic activities of Au@NC were then examined by electrochemical measurements in 0.5 M H_2SO_4. Au@NC possesses apparent non-zero cathodic currents (Figure 4a) as demonstrated by a small onset potential of −54.1 mV (vs. RHE, current density of 1 mA cm^{-2}; Supporting Information, Figure S7). In contrast, pure Au nanoparticles (SEM images; Supporting Information, Figure S8a,b), NC (XPS results; Supporting Information, Figure S9), and Au/NC (Supporting Information, Figure S8c,d) possessed much larger onset potentials of −306, −322.4, and −168 mV versus RHE, respectively. Au/NC samples post-treated at 300 and 900 °C under Ar atmosphere demonstrated lower HER activity than Au@NCs (Supporting Information, Figure S10). The improved HER reactivity from Au@NC might account for the synergetic effect between the Au core and the N-doped carbon shell. However, Au@NC was still inferior to 20 wt% Pt/C (−16 mV). The effects of calcination temperature (700, 800, 900, and 1000 °C; Supporting Information, Figures S11-S13) and Au content (Supporting Information, Figures S14 and S15) on the HER activity were also probed. The findings imply that N-doping and an increased Au core and NC shell interface play an important role in enhancing the HER activity of Au@NC.

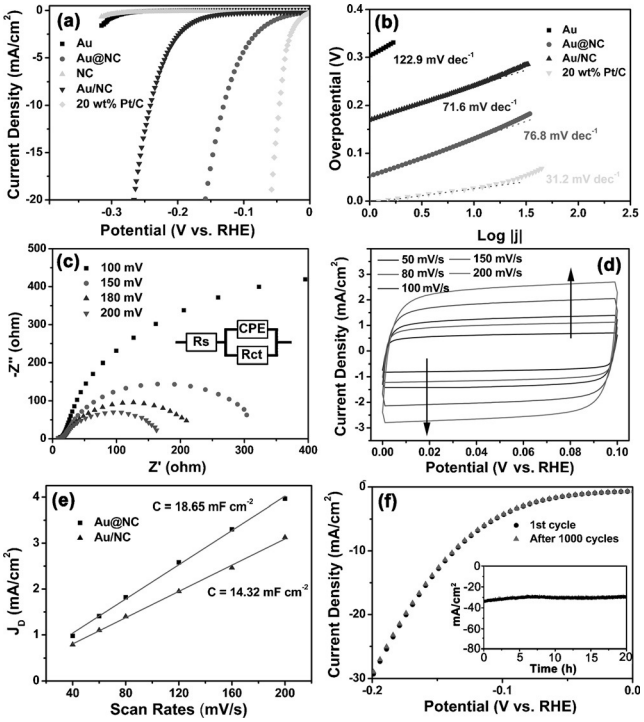

Figure 4. a) Polarization curves for HER in 0.5 M H_2SO_4 on glassy carbon electrodes modified with Au nanoparticles, NC, Au nanoparticles loaded on NC (Au/NC), Au@NC, and 20 wt% Pt/C. b) Corresponding Tafel plots derived from (a). c) Nyquist plots of Au@NC at various overpotentials. d) Cyclic voltammograms without faradaic reactions of Au@NC. e) Variation of double-layer charging currents at +0.05 V with potential scan rate. f) HER polarization curves for Au@NC before and after 1000 cycles. Inset: current-time plots with an overpotential of 300 mV.

As shown in Figure 4b, the Tafel slope of Au@NC is 76.8 mV dec^{-1}, much smaller than that of NC (122.9 mV dec^{-1}) but larger than that of 20 wt% Pt/C (31.2 mV dec^{-1}), which proceeded through a Volmer–Heyrovsky mechanism. Consequently, the electrochemical desorption process is probably the rate-limiting step. The Tafel slope of Au@NC is slightly larger than that of Au/NC (71.6 mV dec^{-1}), suggesting that the electrochemical desorption process is suppressed by the carbon shell. In general, Au@NC possesses enhanced HER performance (−130 mV vs. RHE @10 mA cm^{-2}) compared to that of Au/NC (−242 mV). Additionally, the exchange current density determined from the Tafel plot of Au@NC is 0.186 mA cm^{-2}, which is much larger than that of Au/NC (0.005 mA cm^{-2}; Supporting Information, Figure S16). The typical Nyquist plots obtained from the electrochemical impedance spectroscopic (EIS) response of Au@NC show that the diameter of the semicircles decreased with an increase of overpotential, from 892.4 Ω at 100 mV to 168 Ω at 200 mV (Figure 4c). The remarkable HER performance of Au@NC (onset potential of −54.1 mV vs. RHE, 76.8 mV dec^{-1}) was better than, or at least comparable to, those of leading carbon and transition metal-based HER catalysts in 0.5 M H_2SO_4, such as FeCo@NCNTs-NH (−70 mV, 74 mV dec^{-1}),[6a] N/Co-doped PCP//NRGO (−58 mV, 126 mV dec^{-1}),[1d] CoNi@NC (−30 mV, 104 mV dec^{-1}),[7] bacteriorhodopsin/Ag nanoparticle (−63 mV, 170 mV dec^{-1}),[13] atomic Co on N-doped graphene (−30 mV, 82 mV dec^{-1}),[14] and MoS_2/dealloyed nanoporous gold (−125 mV, 41 mV dec^{-1}).[15] A detailed comparison of electrocatalysts is provided in Table S1 (see the Supporting Information).

Cyclic voltammetry (CV) was employed to measure the electric double-layer capacitance of Au@NC and Au/NC-modified electrodes at the solid–liquid interface, which is an important parameter for estimating the electrochemically active surface area (Figure 4d). The double-layer capacitance of Au@NC (18.65 mF cm^{-2}) was similar to that of Au/NC (14.32 mF cm^{-2}), as exhibited in Figure 4e. Even after application of corrections that take electrochemical surface area into account, the HER performance of Au@NC was still much better than that of Au/NC (Supporting Information, Figure S17), implying that electrochemical surface area is not the dominant factor responsible for enhanced HER activity. Notably, the Au in Au@NC possessed much higher activity than that in Au/NC and Au (Supporting Information, Figure S18), leading to enhanced catalytic activity.

Figure 4f displays the polarization curves before and after 1000 cycles of continuous CV scans, and chronopotentiometry measurement of Au@NC. The current density was nearly constant after 20 h of testing at an operating overpotential of 300 mV, indicating good durability of the catalyst in acidic electrolyte. Bubbles observed on the electrode surface were confirmed to be H_2 by gas chromatography. The production

rate of H_2 was determined to be 961.6 mmol g^{-1} h^{-1} after linear fitting of the experimental data (Supporting Information, Figure S19).

Interestingly, as a multifunctional electrocatalyst, Au@NC also exhibited electrocatalytic activity for ORR in alkaline media (Supporting Information, Figures S20–S22). Au@NC displayed superior ORR performance (+0.97 V vs. RHE, $n \approx 3.86$ at 0.7 V) compared to Au nanoparticles (+0.71 V, $n \approx 3.54$), NC (+0.83 V, $n \approx 3.62$), and Au/NC (+0.87 V, $n \approx 3.77$); Au@NC performed similarly when compared to 20 wt% Pt/C catalysts (+0.97 V, $n \approx 3.94$). Generally speaking, ORR and HER performances followed the same trend. More importantly, Au@NC also showed excellent durability and tolerance toward methanol crossover. The ORR performance of Au@NC was better than those of reported Au-based ORR catalysts, such as Au cluster/graphene (−0.08 V vs. Ag/AgCl, $n \approx 3.6$),[8a] and gold nanodendrites on graphene oxide nanosheets (half-wave potential of +0.61 V vs. RHE, $n = 3.7$).[16]

The aforementioned results reveal a simple and straightforward strategy for recovering precious metals using a microorganism to fabricate valuable electrocatalysts with HER and ORR functionality. The remarkable catalytic activity of Au@NC may be attributed to the following factors. Firstly, the carbon derived from microorganism cells exhibits a large electrochemically active area. Moreover, N-doping within the graphitic matrix led to the formation of active sites for proton and oxygen adsorption.[17] Secondly, the in situ bioreduction of Au inside microorganism cells, and the subsequent calcination process, produced strong interactions between Au and the carbon substrate, which was advantageous for charge transfer. Herein, we describe our observations of chemical reactions (Supporting Information, Figure S6) and electron transfer (Figure 3 d) between the Au core and carbon shell. In general, it is difficult to chemically bond the inert Au atom with other atoms. Theoretical calculations reveal that defects caused by N-doped carbon promote bonding between Au and carbon atoms (Supporting Information, Figure S23). Finally, the electronic density states of N-doped carbon substrate were modulated by Au nanoparticles, which promoted additional catalytic activity.[18] Note that similar mechanisms are extensively reported in transition metal@carbon systems for HER, such as Co@NC and FeCo@NC.[7,19]

In summary, evenly dispersed gold nanoparticles (ca. 20 nm) embedded in N-doped carbon (Au@NC) were derived after bioreduction of precious metals by microorganism cells. The obtained Au@NC was employed as an efficient and multifunctional electrocatalyst for HER and ORR. HRTEM images and XPS results confirm the strong interaction and charge transport between the Au core and N-doped carbon generated by the in situ bioreduction and calcination process. Electrochemical measurements indicate that Au@NC displays efficient HER activity with a small onset potential of only −54.1 mV (vs. RHE), a Tafel slope of 76.8 mV dec^{-1}, a large catalytic current density, and electrochemical durability. Moreover, Au@NC displayed efficient catalytic activity for ORR (0.97 V vs. RHE, $n \approx 3.86$) and tolerance toward methanol crossover. The results presented herein may offer a simple and effective method for the reclamation of precious metals from waste electronic equipment, allowing large scale preparation of efficient and multifunctional electrocatalysts for HER and ORR.

Acknowledgements

This work was supported by the National Recruitment Program of Global Experts, Project of Public Interest Research and Capacity Building of Guangdong Province (2014A010106005), the Fundamental Research Funds for the Central Universities (201522103) and the National Natural Science Foundation of China (51502096, 31272482, 51178191).

Keywords: biosynthesis · core–shell structure · electron transfer · hydrogen evolution reaction · catalyst recycling

How to cite: *Angew. Chem. Int. Ed.* **2016**, *55*, 8416–8420
Angew. Chem. **2016**, *128*, 8556–8560

[1] a) J. Luo, J.-H. Im, M. T. Mayer, M. Schreier, M. K. Nazeeruddin, N.-G. Park, S. D. Tilley, H. J. Fan, M. Grätzel, *Science* **2014**, *345*, 1593–1596; b) R. Sathre, C. D. Scown, W. R. Morrow, J. C. Stevens, I. D. Sharp, J. W. Ager, K. Walczak, F. A. Houle, J. B. Greenblatt, *Energy Environ. Sci.* **2014**, *7*, 3264–3278; c) R. Subbaraman, D. Tripkovic, D. Strmcnik, K.-C. Chang, M. Uchimura, A. P. Paulikas, V. Stamenkovic, N. M. Markovic, *Science* **2011**, *334*, 1256–1260; d) Y. Hou, Z. Wen, S. Cui, S. Ci, S. Mao, J. Chen, *Adv. Funct. Mater.* **2015**, *25*, 872–882; e) S. Bai, C. Wang, M. Deng, M. Gong, Y. Bai, J. Jiang, Y. Xiong, *Angew. Chem. Int. Ed.* **2014**, *53*, 12120–12124; *Angew. Chem.* **2014**, *126*, 12316–12320.

[2] X. Fan, Z. Peng, R. Ye, H. Zhou, X. Guo, *ACS Nano* **2015**, *9*, 7407–7418.

[3] a) W. Zhou, K. Zhou, D. Hou, X. Liu, G. Li, Y. Sang, H. Liu, L. Li, S. Chen, *ACS Appl. Mater. Interfaces* **2014**, *6*, 21534–21540; b) D. Gopalakrishnan, D. Damien, M. M. Shaijumon, *ACS Nano* **2014**, *8*, 5297–5303; c) W. Zhou, D. Hou, Y. Sang, S. Yao, J. Zhou, G. Li, L. Li, H. Liu, S. Chen, *J. Mater. Chem. A* **2014**, *2*, 11358–11364.

[4] J. Tian, Q. Liu, A. M. Asiri, X. Sun, *J. Am. Chem. Soc.* **2014**, *136*, 7587–7590.

[5] a) X. Zou, X. Huang, A. Goswami, R. Silva, B. R. Sathe, E. Mikmekova, T. Asefa, *Angew. Chem. Int. Ed.* **2014**, *53*, 4372–4376; *Angew. Chem.* **2014**, *126*, 4461–4465; b) T. Wang, Q. Zhou, X. Wang, J. Zheng, X. Li, *J. Mater. Chem. A* **2015**, *3*, 16435–16439; c) M. Tavakkoli, T. Kallio, O. Reynaud, A. G. Nasibulin, C. Johans, J. Sainio, H. Jiang, E. I. Kauppinen, K. Laasonen, *Angew. Chem. Int. Ed.* **2015**, *54*, 4535–4538; *Angew. Chem.* **2015**, *127*, 4618–4621.

[6] a) J. Deng, P. Ren, D. Deng, L. Yu, F. Yang, X. Bao, *Energy Environ. Sci.* **2014**, *7*, 1919–1923; b) J. Deng, L. Yu, D. Deng, X. Chen, F. Yang, X. Bao, *J. Mater. Chem. A* **2013**, *1*, 14868–14873; c) J. Duan, S. Chen, M. Jaroniec, S. Z. Qiao, *ACS Nano* **2015**, *9*, 931–940; d) Y. Ito, W. Cong, T. Fujita, Z. Tang, M. Chen, *Angew. Chem. Int. Ed.* **2015**, *54*, 2131–2136; *Angew. Chem.* **2015**, *127*, 2159–2164.

[7] J. Deng, P. Ren, D. Deng, X. Bao, *Angew. Chem. Int. Ed.* **2015**, *54*, 2100–2104; *Angew. Chem.* **2015**, *127*, 2128–2132.

[8] a) H. Yin, H. Tang, D. Wang, Y. Gao, Z. Tang, *ACS Nano* **2012**, *6*, 8288–8297; b) S. Guo, X. Zhang, W. Zhu, K. He, D. Su, A.

Mendoza-Garcia, S. F. Ho, G. Lu, S. Sun, *J. Am. Chem. Soc.* **2014**, *136*, 15026 – 15033; c) S.-S. Kim, Y.-R. Kim, T. D. Chung, B.-H. Sohn, *Adv. Funct. Mater.* **2014**, *24*, 2764 – 2771; d) L. Wang, Z. Tang, X. Liu, W. Niu, K. Zhou, H. Yang, W. Zhou, L. Li, S. Chen, *RSC Adv.* **2015**, *5*, 103421 – 103427.

[9] a) Z. Zhuang, W. Sheng, Y. Yan, *Adv. Mater.* **2014**, *26*, 3950 – 3955; b) B. S. Yeo, A. T. Bell, *J. Am. Chem. Soc.* **2011**, *133*, 5587 – 5593.

[10] M. K. Kundu, T. Bhowmik, S. Barman, *J. Mater. Chem. A* **2015**, *3*, 23120 – 23135.

[11] a) B. O. Okesola, S. K. Suravaram, A. Parkin, D. K. Smith, *Angew. Chem. Int. Ed.* **2016**, *55*, 183 – 187; *Angew. Chem.* **2016**, *128*, 191 – 195; b) S. K. Das, J. Liang, M. Schmidt, F. Laffir, E. Marsili, *ACS Nano* **2012**, *6*, 6165 – 6173; c) L. Fairbrother, B. Etschmann, J. Brugger, J. Shapter, G. Southam, F. Reith, *Environ. Sci. Technol.* **2013**, *47*, 2628 – 2635.

[12] Q. Liu, X. Yang, Y. Huang, S. Xu, X. Su, X. Pan, J. Xu, A. Wang, C. Liang, X. Wang, T. Zhang, *Energy Environ. Sci.* **2015**, *8*, 3204 – 3207.

[13] Z. Zhao, P. Wang, X. Xu, M. Sheves, Y. Jin, *J. Am. Chem. Soc.* **2015**, *137*, 2840 – 2843.

[14] H. Fei, J. Dong, M. J. Arellano-Jimenez, G. Ye, N. Dong Kim, E. L. G. Samuel, Z. Peng, Z. Zhu, F. Qin, J. Bao, M. J. Yacaman, P. M. Ajayan, D. Chen, J. M. Tour, *Nat. Commun.* **2015**, *6*, 8668.

[15] X. Ge, L. Chen, L. Zhang, Y. Wen, A. Hirata, M. Chen, *Adv. Mater.* **2014**, *26*, 3100 – 3104.

[16] X. Li, X. Li, M. Xu, J. Xu, H. Chen, *J. Mater. Chem. A* **2014**, *2*, 1697 – 1703.

[17] a) Y. Zhou, Y. Leng, W. Zhou, J. Huang, M. Zhao, J. Zhan, C. Feng, Z. Tang, S. Chen, H. Liu, *Nano Energy* **2015**, *16*, 357 – 366; b) Z. Wen, S. Ci, Y. Hou, J. Chen, *Angew. Chem. Int. Ed.* **2014**, *53*, 6496 – 6500; *Angew. Chem.* **2014**, *126*, 6614 – 6618; c) W. Niu, L. Li, X. Liu, N. Wang, J. Liu, W. Zhou, Z. Tang, S. Chen, *J. Am. Chem. Soc.* **2015**, *137*, 5555 – 5562.

[18] J. Lu, W. Zhou, L. Wang, J. Jia, Y. Ke, L. Yang, K. Zhou, X. Liu, Z. Tang, L. Li, S. Chen, *ACS Catal.* **2016**, *6*, 1045 – 1053.

[19] W. Zhou, Y. Zhou, L. Yang, J. Huang, Y. Ke, K. Zhou, L. Li, S. Chen, *J. Mater. Chem. A* **2015**, *3*, 1915 – 1919.

Received: March 15, 2016
Revised: April 12, 2016
Published online: May 24, 2016

